

EFFECT OF ULTRASONIC IRRADIATION TIME AND AMPLITUDE VARIATION ON TiO₂ PARTICLES

Radhiyah A. Aziz, Norhanita M. Yusof and Abdul K. Masrom*

*Industrial Nanotechnology Research Center, SIRIM Berhad, Lot 34,
Jalan Hi-Tech 2/3, Kulim Hi-Tech Park, 09000 Kulim, Kedah*

**Corresponding author: akadir@sirim.my*

ABSTRACT

A novel sonochemical method has been applied to directly prepare TiO₂ colloid. TiO₂ colloids were synthesized by using titanium tetraisopropoxide as a precursor of titanium. Ultrasonic irradiation was applied during the reaction process of the reactants. Several variable parameters of ultrasonic irradiation were applied upon the TiO₂ colloid (ultrasonic irradiation time and amplitude). Then, TiO₂ colloids were used to fabricate TiO₂ thin film via dip coating process. The TiO₂ thin films were then calcined at 500 °C for 2 hours. The physical and chemical properties of TiO₂ thin film were studied using different techniques of characterization such as X-ray diffraction (XRD), Transmission Electron Microscope (TEM), and UV-Vis spectrophotometer. It seems that increasing ultrasonic irradiation amplitude leads to the formation of bigger TiO₂ particles in the colloid as confirmed by the shift of absorption edge towards shorter wavelength and TEM pictures. The efficiency of TiO₂ thin film photocatalyst was evaluated on degradation of methylene blue.

Keywords: Sonochemical; amplitude; TiO₂; photocatalyst;

INTRODUCTION

Semiconductor photocatalysis with a primary focus on TiO₂ as a durable photocatalyst has been applied to a variety of problems of environmental interest in addition to water and air purification [1]. Its ability to initiate the photocatalytic activity and degrade most of the organic pollutant molecules in environment has been proved [1, 2]. Even though there are a lot of semiconductors that can be functioned as photocatalyst, the ability of TiO₂ still is the most promising and useful photocatalyst for the destruction of microorganisms and organic contaminants such as bacteria and viruses [3, 4], inactivation of cancer cells [5], air purification [6-8] and water treatment [9-11].

It is well established that particle size is one of the most important parameters to be optimized for improving the catalytic or photocatalytic properties of a semiconductor [11]. Small particles affect photocatalytic properties by increasing the number of active surface sites in contact with the organic pollutant molecules to be photocatalytically

degraded. It also can lead to the less risk of charge carrier recombination [12, 13].

Nowadays, a number of promising synthesis routes that can influence the physico-chemical properties of the nanoparticulate TiO_2 materials are available. Such physico-structural parameters include crystallization degree, crystal shape, surface area, as well as the eventual presence of a secondary rutile phase [1]. Nanoparticulate materials can be prepared by one of the three methods via; solid state, solution state and vapor phase deposition [14]. One of the examples of solution state method is via sonochemical synthesis.

Sonochemistry is the application of ultrasound to chemical reactions and processes. This method is capable of creating extreme conditions inside a cavitating bubble, sponsoring cavitation to occur, and have shown positive effects to produce a variety of nanostructured materials. Sonochemical synthesis route is a versatile method that can be satisfactorily used to produce nanostructured materials with different physical and chemical characteristics just by changing the treatment condition (e.g., ultrasonic irradiation time, amplitude, temperature) [15, 16]. Besides, ultrasonic irradiation route could enhance the rate of reaction for many homogeneous and heterogeneous chemical reactions [17].

In this present study, TiO_2 colloids were synthesized via hydrolysis and polycondensation route using titanium tetraisopropoxide (TPT) as a metal alkoxide precursor. Ultrasonic treatment was applied during the reaction of synthesizing the TiO_2 colloid. The TiO_2 colloids were then used to fabricate TiO_2 thin film and calcined at $500\text{ }^\circ\text{C}$ for 2 hours. Physico-chemical property of the TiO_2 thin film obtained has been also carried out to investigate the effect of different ultrasonic irradiation amplitude and time use in changing the TiO_2 particles in the colloid. Then, methylene blue has been selected as representative of organic compound to be photodegraded by TiO_2 thin film photocatalyst in order to evaluate its photocatalytic performance.

EXPERIMENTAL DETAILS

For preparation of TiO_2 colloid, titanium (IV) isopropoxide (TPT, Sigma-Aldrich), isopropanol, diethanolamine (DEA), hydrochloric acid (HCl) and deionized water (DIW) were used as raw materials. The weight composition of each raw material was summarized in Table 1. The mixture is then subjected to sonication using an ultrasonic processor VCX750 with 20 kHz at various amplitudes delivering different power depending on amplitude. The ultrasonic irradiation was carried out for various ultrasonic irradiation times with a fixed pulse mode (20s ON and 5s OFF mode). The procedures were summarized in the flowchart (Figure 1).

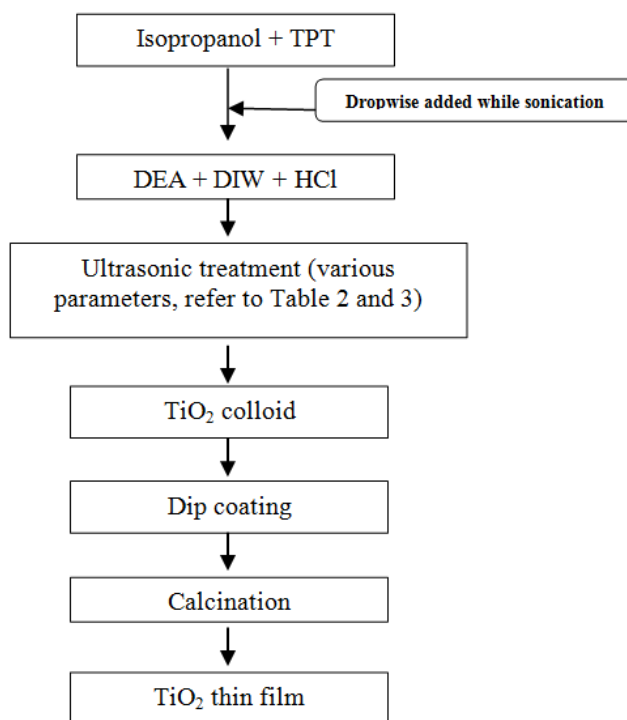


Figure 1: Scheme of TiO₂ thin film via sonochemical method

Table 1: Weight composition of materials used

Sample	TPT (ml)	Isopropanol (ml)	DEA (ml)	DIW (ml)	HCl (ml)
A	10	50	5	40	50

Crystal structure of TiO₂ thin film was characterized using Bruker XRD model with copper K α radiation. All samples were scanned between 20° and 60° with 2.00 °/min scan rate. Particle size of TiO₂ in colloid was measured using Transmission Electron Microscope (TEM). Absorption edge of TiO₂ thin film sample was recorded using UV-Vis spectrophotometer (Perkin Elmer UV-VIS, Lambda 25) in the range of 300 - 800 nm.

Photocatalytic assessment of the TiO₂ thin film was done by decolorizing methylene blue under UV irradiation (280 nm). The TiO₂ thin films were placed in a container and filled with the 25 ml of methylene blue. Concentration of the methylene blue was varied at 3 and 5 ppm. This container was then placed in the closed photoreactor to be irradiated with UV lamp. The UV light was irradiated for 180 minutes. The sampling was done every 30 minutes and the change in absorbance and concentration of methylene blue was determined using UV-Vis spectrophotometer.

Table 2: Variation of ultrasonic amplitude

Amplitude (%)	ultrasonic irradiation time (min)	Sample Name
30	60	A30
40	60	A40
50	60	A50
60	60	A60
70	60	A70

Table 3. Variation of ultrasonic irradiation time

Sample Name	Amplitude (%)	Irradiation Time(min)
A40T60	40	60
A40T90	40	90
A40T120	40	120
A40T180	40	180

RESULT AND DISCUSSION

Crystallinity and particle size of the TiO₂ thin film was analyzed using XRD machine. This characterization step was done to investigate the effect of various ultrasonic irradiation times and amplitudes of ultrasonic applied upon the crystal structure and particle size of TiO₂. TiO₂ thin film was fabricated using TiO₂ colloids which were derived from different condition of ultrasonic treatment applied (Table 2 and Table 3). All the thin film samples were calcined at 500 °C for 2 hours. Therefore, condition of calcination process will not affect the crystallinity and particle size of TiO₂.

Figure 2(a, b, c, d and e) showed XRD patterns of TiO₂ thin films which were fabricated under different ultrasonic irradiation time with the ultrasonic amplitude of 30, 40, 50, 60 and 70 %, respectively. As shown in Figure 2, it can be seen the presence of anatase characteristic peak for all samples. However, there is a new characteristic peak appeared for sample A70 which is assigned to the rutile phase. The intensity of anatase characteristic peak for A30 sample is lower than that of A70 sample. It can be inferred that the crystallinity of the TiO₂ particles increased as the ultrasonic irradiation amplitude increased from 30 % up to 70 %. It is due to more heat energy supplied to the TiO₂ particles as the amplitude increased that favorable for crystal growth. Besides, the increase of this peak intensity showed a marked increase of the peak breadth for other sample. Thus, the presence of bigger TiO₂ particle was observed for sample synthesized using high ultrasonic amplitude. This result can be supported by TEM analysis.

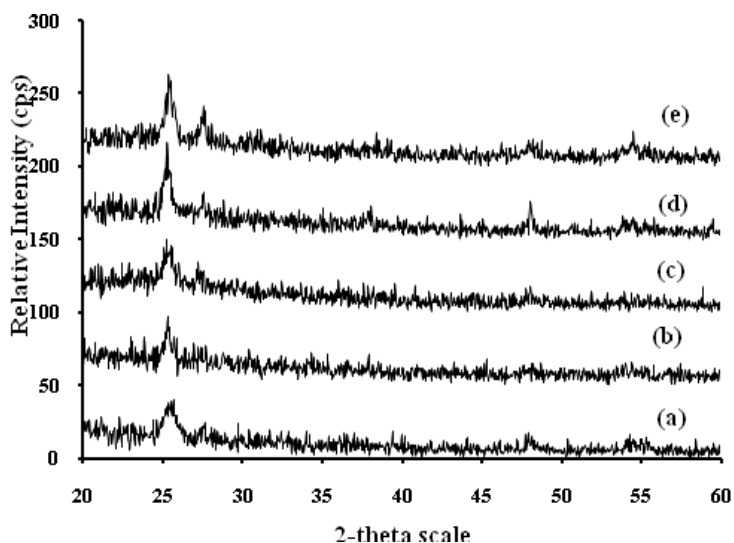


Figure 2: XRD patterns of TiO₂ thin film; (a) A30, (b) A40, (c) A50, (d) A60 and (e) A70

As the ultrasonic irradiation time increased, the intensity of the anatase characteristic peak increased. It is due to more dispersed TiO₂ particles that favorable for crystal growth. And it may be attributed to the high temperature build up due to the continuation of ultrasonic irradiation time to the reaction medium. Besides, the TiO₂ particles seem to form bigger particles. This can be supported by the XRD patterns (Figure 3a, 3b, 3c and 3d) as the peak breadth become narrower.

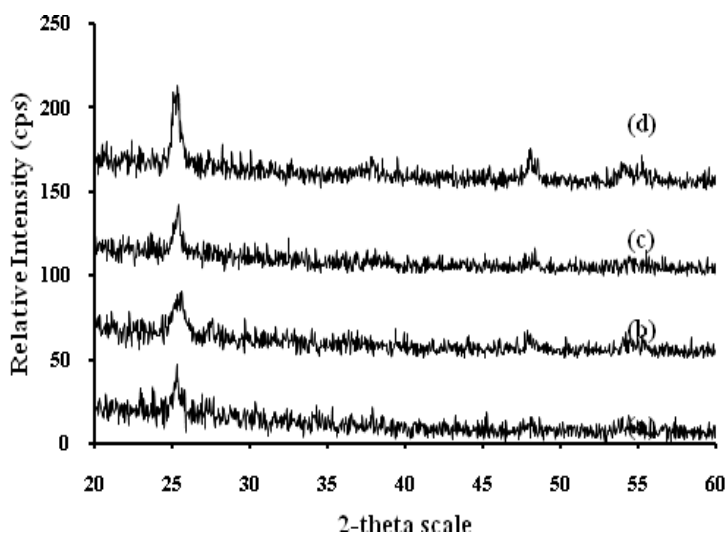


Figure 3: XRD patterns of TiO₂ thin film; (a) A40T60, (b) A40T90, (c) A40T120 and (d) A40T180

Figure 4 showed TEM pictures of TiO₂ particles in the colloid form. The TiO₂ colloids were synthesized with different ultrasonic irradiation time and amplitude. From the figure, it can be observed that an increased of ultrasonic amplitude from 30 % to 70% leads to the formation of larger size of TiO₂ particles. The individual TiO₂ particles of these samples tend to agglomerate and form bigger particles with non-spherical shape as the ultrasonic amplitude increased. However, this occurrence only appeared for the TiO₂ colloids which were derived by higher amplitude value (60 and 70 %) as it encouraging extensive agglomeration amongst particles [14].

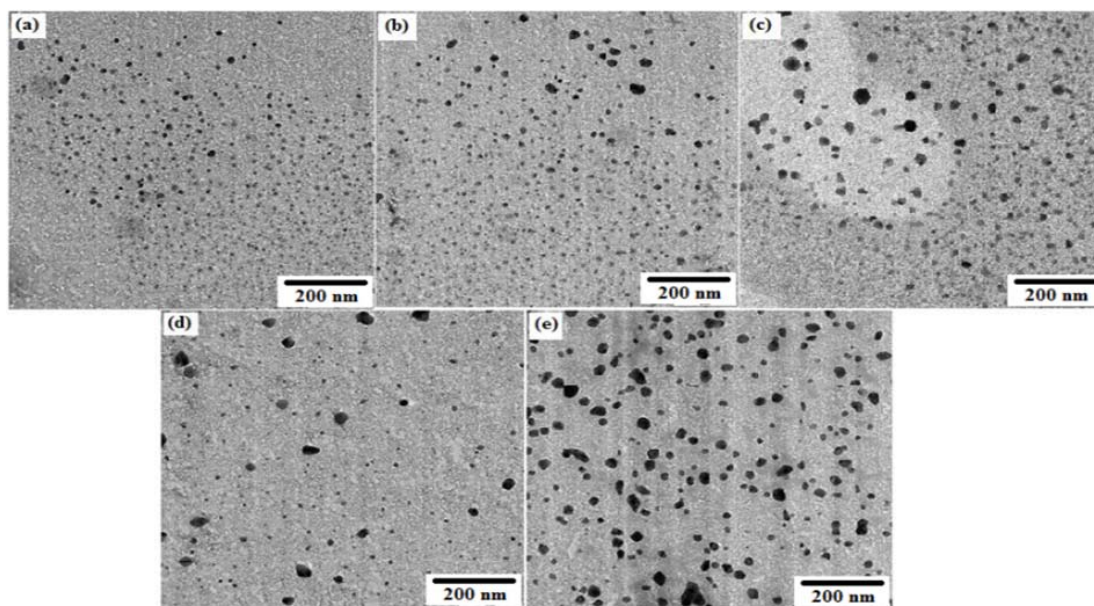


Figure 4: TEM picture of TiO₂ particles; (a) A30, (b) A40, (c) A50, (d) A60, and (e) A70

In certain condition, prolongation of ultrasonic irradiation time was favorable for the fragmentation the TiO₂ particles and also increased high velocity interparticle collisions among the particles, in turn avoiding the formation of larger TiO₂ particles [18]. However, different occurrence has been observed in this experiment. As the ultrasonic irradiation time increased, the TiO₂ particles tend to form bigger particles as can be seen in the Figure 5. It may be due to the continuous ultrasonic irradiation provides higher local temperatures that are a consequence of low energy cavity collapse due to acoustic cavitation. Thus, there is bigger particles of TiO₂ was observed for sample synthesized under longer ultrasonic irradiation time.

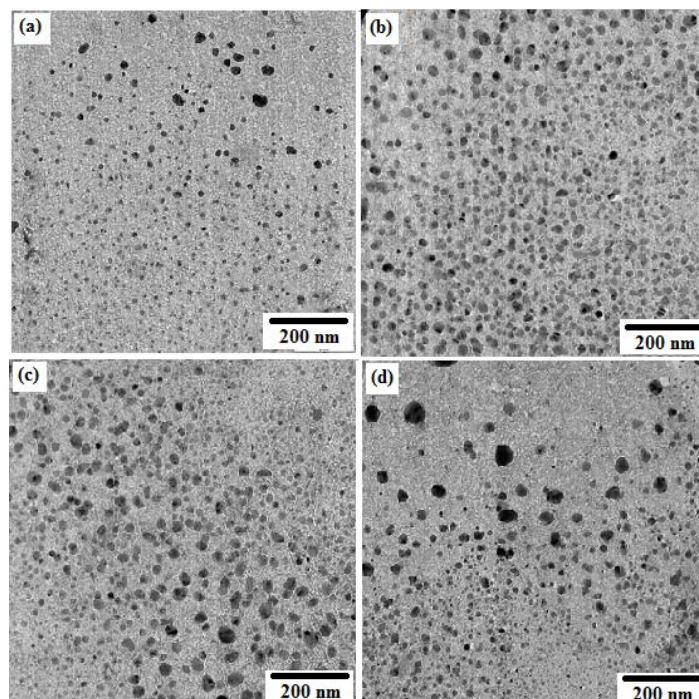


Figure 5: TEM pictures of TiO₂ nanoparticles in colloid; (a) A40T60, (b) A40T90, (c) A40T120 and (d) A40T180

Figure 6 and 7 showed the UV-Vis transmittance spectra of TiO₂ thin film deposited on the glass substrate which were derived from different TiO₂ colloids. The spectra exhibited higher transmittance ($\approx 100\%$) with considerable absorption in the visible region. When the particles of the sample are exposed to the light having an energy that matches a possible electronic transition within the particles, some of the light energy will be absorbed as the electron is promoted to a higher energy orbital. Thus, this UV-Vis spectrophotometer records the wavelengths at which absorption occurs for the thin film photocatalyst activate the photocatalytic reaction.

From Figure 6, it was observed that absorption edge of all thin film samples started at ~ 290 - 315 nm and this absorption edge shifted towards shorter wavelengths with increase in the ultrasonic amplitude during synthesis of the TiO₂ colloids. Table 4 summarized the change of absorption edge and band gap energy as the ultrasonic amplitude change. The shift can be ascribed to the difference in particle size [19-21]. The presence of bigger TiO₂ particle is due to the high value of ultrasonic amplitude. This result is corroborated with the XRD and TEM analysis.

Figure 7 showed the optical absorbance of TiO₂ thin films which were derived from constant ultrasonic amplitude with the different ultrasonic irradiation time. It can be seen that as the ultrasonic irradiation time applied increase, the absorption edge shifted towards shorter wavelength. Table 5 summarized the change of absorption edge with

calculated band gap energy as the ultrasonic irradiation time change. It may be attributed to the presence of larger TiO₂ particles on the thin film since longer ultrasonic irradiation time promoting larger particle size. This result is corroborated with the TEM and XRD analysis.

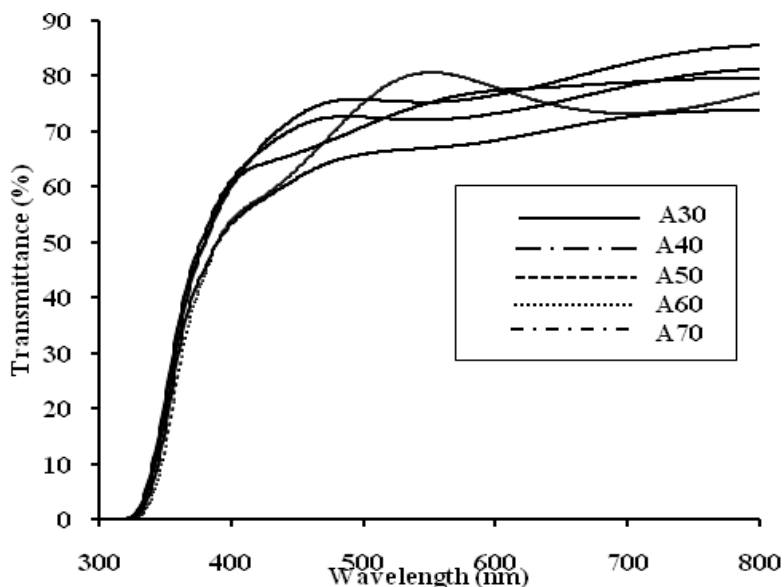


Figure 6: UV-Vis spectra of TiO₂ thin film derived using different amplitude with a constant ultrasonic irradiation time

Table 4: Optical parameters for the TiO₂ thin film

Sample	Absorption edge (nm)	Band Gap Energy (eV)
A30	475	2.61
A40	465	2.67
A50	413	3.01
A60	409	3.04
A70	406	3.06

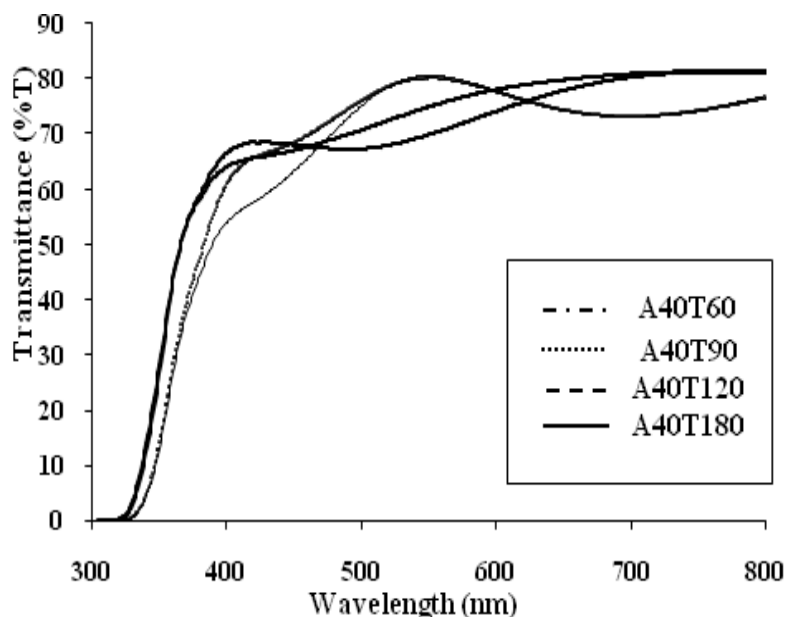


Figure 7: Optical absorbance spectra of TiO₂ thin film derived using constant amplitude with different ultrasonic irradiation time

Table 5: Optical parameters of TiO₂ thin film

Sample	Absorption edge (nm)	Band Gap Energy (eV)
A40T60	426	2.91
A40T90	422	2.94
A40T120	411	3.02
A40T180	405	3.07

Photocatalytic performance of TiO₂ thin film sample has been investigated by measuring the change in color of methylene blue as a function of UV irradiation time. Decoloration of the dye indicates that it has been photodegraded in the reaction. The methylene blue absorption showed in Figure 8 highlights the phenomenon of methylene blue degradation by the TiO₂ thin film sample. As can be seen, the intensity of the absorption peak at 665 nm decreases progressively according to the time of irradiation.

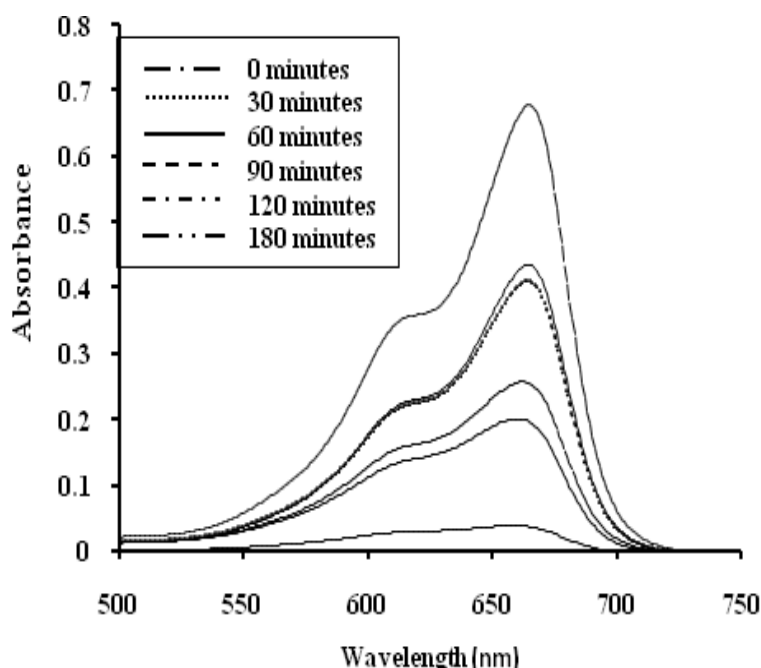


Figure 8: Absorbance spectra of 5 ppm methylene blue photodegraded by TiO₂ thin film (A30)

Figure 9 showed the methylene blue concentration (3 and 5ppm) as a function of irradiation time for A30 and A70 thin film sample. From the slope of the graph, it showed that the A30 thin film sample has higher rate in degrading the methylene blue either in low or high concentration. The result deduced that the drastic decrease in concentration of methylene blue was correlated to the crystalline phase and the presence of smaller TiO₂ particles of A30 thin film sample. It is established that crystalline phase of TiO₂ could lead to the most active of charge carrier generation. So, more oxidizing and reducing agent (O₂[•] and •OH) will be highly produced. These generated radicals are the principal agents responsible for the oxidation of numerous aqueous organic contaminants [22]. It is also noteworthy to mention that the presence of smaller TiO₂ particles lead to the higher rate in degrading the methylene blue as it has higher surface area for the molecules adsorption occurred [23].

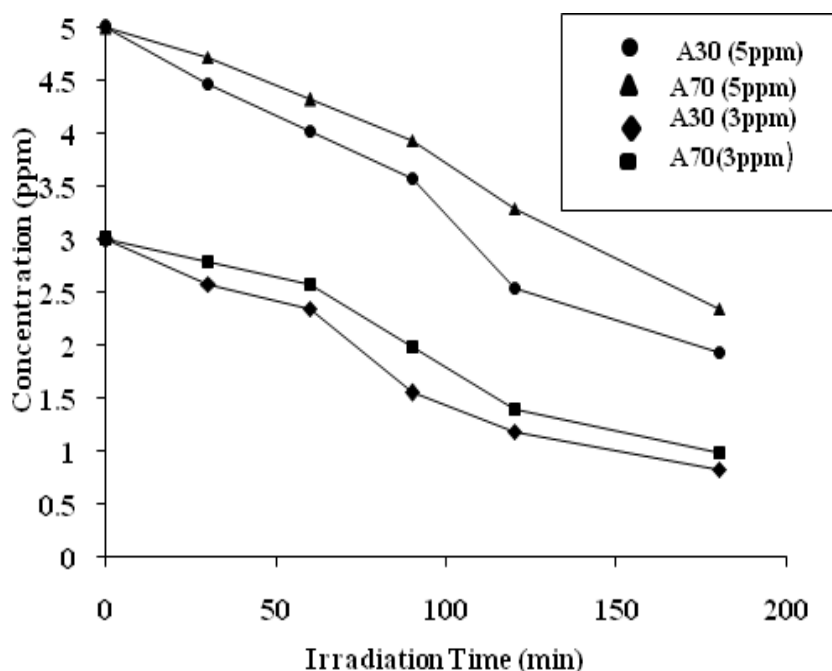


Figure 9: Graph of concentration vs. irradiation time on photodegradation of various concentration methylene blue using different TiO₂ thin film

CONCLUSION

TiO₂ colloids photocatalyst have been successfully synthesized via sonochemical route and have been used as a precursor to fabricate TiO₂ thin film photocatalyst. The effects of different ultrasonic treatment condition on the physical and chemical property have been investigated. XRD and TEM analysis revealed that the individual TiO₂ particles of these samples tend to agglomerate and form bigger particles with non-spherical shape as the ultrasonic amplitude increased. Besides, the formation of agglomerated TiO₂ particles is also attributed to the prolongation of ultrasonic irradiation time. From photocatalytic experiment, it can be concluded that A30 sample has higher rate photocatalytic activity than that of A70. It is believed due to the presence of smaller size TiO₂ particles with a high crystallinity of the thin film photocatalyst.

ACKNOWLEDGEMENT

The authors thank the Ministry of Science, Technology and Innovation (MOSTI) for its financial support through a research project no.: 03-03-02-SF0106.

REFERENCES

- [1] M. R. Hoffmann, S. T. Martin, W. Choi, D. W. Bahnemann, *Chemicals Reviews* **95** (1995) 69-96
- [2] Y. V. Kolen'ko, B. R. Churagulov, M. Kunst, L. Mazerolles, C. C. Justin, *Applied Catalysis B: Environmental*. **54** (2004) 51-58
- [3] K. Sunada, T. Watanabe, K. Hashimoto, *Environmental Science & Technology*. **37**(20) (2003) 4785-4789
- [4] S. Q. Sun, B. Sun, W. Zhang, D. Wang, *Buletin of Materials Science*. **31**(1) (2008) 61-66
- [5] A. Fujishima, T. N. Rao, D. A. Tryk, *Journal of Photochemistry and Photobiology C: Photochemistry Reviews*. **1** (2000) 1-21
- [6] I. Sopyan, M. Watanabe, S. Murasawa, K. Hashimoto, A. Fukishima, *Journal Photochemistry and Photobiology Part A: Chemistry*. **98** (1996) 79-86
- [7] Y. Chiba, H. Kokai, K. Kashiwagi, *Journal of Materials Science: Materials in Electronics*. **16** (2005) 645-648
- [8] T. Watanabe, S. Fukayama, M. Miyauchi, A. Fujishima, K. Hashimoto, *Journal of Sol-Gel Science and Technology*. **19** (2000) 71-76
- [9] L. Zhou, S. Yan, B. Tian, J. Zhang, M. Anpo, *Materials Letter*. **60** (2006) 396-399
- [10] S. Stoyanov, D. Mladenova, C. Dushkin, *React. Kinet. Catal. Lett*. **88**(2) (2006) 277-283
- [11] M. Fallet, S. Permpoon, J. L. Deschanvres, M. Langlet, *Journal of Materials Science*. **74** (2006) 2915-2927
- [12] D. Beydoun, R. Amal, G. Low, S. McEvoy, *Journal of Nanoparticle Research*. **1** (1999) 439-458
- [13] T. Hanley, Y. Krisnandi, A. Eldewik, V. Luca, R. Howe, *Ionics*. **7** (2001) 319-326
- [14] K. Prasad, D. V. Pinjari, A. B. Pandit, S. T. Mhaske, *Ultrasonics Sonochemistry*. **17** (2010) 697-703
- [15] L. G. Reyes, I. Hernández-Pérez, F. C. Robles Hernández, H.D. Rosales, E. M. Arce-Estrada, *Journal of the European Ceramic Society*. **28** (2008) 1585-1594
- [16] B. Tian, F. Chen, J. Zhang, M. Anpo, *Journal of Colloid and Interface Science*. **303** (2006) 142-148
- [17] J. C. Yu, J. Yu, L. Zhang, W. Ho, *Journal of Photochemistry and Photobiology A: Chemistry*. **148** (2002) 263-271
- [18] B. Neppolian, Q. Wang, H. Jung, H. Choi, *Ultrasonics Sonochemistry*. **15** (2008) 649-658
- [19] M. Addamo, V. Augugliaro, A. Di Paola, E. Garcia-Lopez, V. Loddo, G. Marci, L. Palmisano, *Thin Solid Films*. **516** (12) (2007) 3802-3807
- [20] M. Takeuchi, H. Yamashita, M. Matsuoka, M. Anpo, T. Hirao, N. Itoh, N. Iwamoto, *Catalysis Letter*. **66** (2000) 185-187
- [21] Y. Zhang, J. Wang, J. Li, *Journal of Electroceramics*. **16** (2006) 499-502
- [22] N. A. Laoufi, D. Tassalit, F. Bentahar, *Global NEST Journal*. **10**(3) (2008) 404-418

- [23] H. Zhang, R. L. Penn, R. J. Hamers, J. F. Banfield, *Journal of Physical Chemistry B*, **103** (1999) 4656-4662